TITLE

Distinct components of photoperiodic light are differentially encoded by the mammalian circadian clock

AUTHORS

Michael C. Tackenberg[1], Jacob J. Hughey[2,3], and Douglas G. McMahon[1,2*]

[1]Vanderbilt Brain Institute, Vanderbilt University, Nashville, TN, USA

[2]Department of Biological Sciences, Vanderbilt University, Nashville, TN, USA

[3]Department of Biomedical Informatics, Vanderbilt University School of Medicine, Nashville, TN, USA

Correspondence: douglas.g.mcmahon@vanderbilt.edu

RUNNING TITLE

Components of photoperiodic light

[*] Lead Contact

ABSTRACT

Seasonal light cycles influence multiple physiological functions and are mediated through photoperiodic encoding by the circadian system. Despite our knowledge of the strong connection between seasonal light input and downstream circadian changes, less is known about the specific components of seasonal light cycles that are encoded and induce persistent changes in the circadian system. Using combinations of three T cycles (23, 24, 26 hr.) and two photoperiods per T cycle (Long and Short, with duty cycles scaled to each T cycle), we investigate after-effects of entrainment to these six light cycles on locomotor behavior duration (alpha), period, and phase *in vivo,* and SCN *ex vivo* phase distribution, period, and phase in order to refine our understanding of critical light components for influencing particular circadian properties. We find that photoperiod and T cycle period both drive determination of entrained phase angle, and differentially influence after-effects in alpha and period, with photoperiod driving changes in alpha and photoperiod length and T cycle length combining to influence period. Using skeleton photoperiods, we demonstrate that phase angle determination is driven by both parametric and non-parametric components, while changes in alpha are driven non-parametrically. Within the SCN, we find that phase angle of entrainment and phase distribution follow closely with their likely behavioral counterparts (phase and alpha), while also confirming previous reports of free-running period after-effects of gene expression rhythms showing negative correlations with behavioral period after-effects in response to T cycles. We demonstrate that phase distribution changes, thought to underly alpha changes *in vivo*, are induced primarily non-parametrically. Taken together, our results demonstrate distinct components of seasonal light input differentially influence phase, activity duration, and period, and suggest the possibility of separate mechanisms driving the persistent changes in circadian behaviors mediated by seasonal light.

KEYWORDS

INTRODUCTION

The duration of daylight, or photoperiod, represents a predictable and dynamic signal of seasonal change throughout the year across much of the planet. The predictability of this signal is harnessed by organisms to initiate or avoid a variety of biological functions at specific times of year, including reproductive behaviors (Elliott and Goldman, 1981), resource conservation (Bartness et al., 1989; Bartness and Wade, 1984), and migration (Gwinner, 1990). In humans, a variety of disorders and non-communicable diseases have seasonal correlations (Basnet et al., 2016; Oh et al., 2010; Wehr, 2001), with perhaps the most striking seasonal influence being on depression-anxiety behaviors (Koorengevel et al., 2003). Despite clear associations between photoperiodic exposure and physiological function and dysfunction, the roles of specific components of seasonal light cycles that induce those changes are incompletely understood.

One factor critical to our current understanding of the mechanism of photoperiodic induction is the persistence of seasonal changes. Physiological hallmarks of exposure to particular light schedules can be observed, for varying intervals, beyond direct exposure to that light schedule (Pittendrigh and Daan, 1976a). These persistent changes, referred to as after-effects, include characteristic changes to core circadian locomotor behavior patterns in the form of activity duration (alpha), free-running period (tau), and phase angle of entrainment (psi). In nocturnal animals, prior exposure to long photoperiods results in a compressed alpha, a shortened free-running period, and an advanced phase angle of entrainment relative to short photoperiod counterparts (Pittendrigh and Daan, 1976a).

The existence of after-effects suggests that seasonal light cycle information is encoded within the brain in a manner that can persist beyond the interval of direct exposure. The master circadian pacemaker of the brain, the suprachiasmatic nucleus (SCN), likely plays a major role in this encoding, particularly with regards to after-effects in circadian behavior (for review, see Tackenberg and McMahon, 2018). In addition, recent work has identified a distinct non-SCN

target for photoperiodic influence, the peri-habenular area, influencing seasonal response in mood (Fernandez et al., 2018). Like circadian locomotor behavior patterning, the SCN undergoes substantial changes in organization following exposure to different photoperiods, constituting network-level after-effects. These responses include changes in phase dispersal of its constituent neurons, free-running period of SCN gene expression rhythms, and phase angle of entrainment. Prior exposure to long photoperiod has been shown to increase phase distribution of *Period1::Luciferase* (Inagaki et al., 2007), PERIOD2::LUCIFERASE (Buijink et al., 2016), and electrical (VanderLeest et al., 2007) rhythms compared to short photoperiod counterparts. As in locomotor behavior after-effects, we have previously found that prior exposure to long photoperiod shortens the SCN free-running period compared to short photoperiod counterparts (16:8 L:D, Ciarleglio et al., 2011; 20:4 L:D, Evans et al., 2013) while others have found non-significant decreases in SCN period length following exposure to long photoperiod, particularly in the anterior SCN (Buijink et al., 2016; Mickman et al., 2008).

Induction of persistent circadian after-effects is not limited to exposure to changes in the duty cycle of light duration within 24 days (photoperiod). Manipulation of total day length, or T cycle length, also induces after-effects in circadian locomotor behavior with entrainment to short T cycles (cycle lengths less than 24 hours), like exposure to long photoperiods, resulting in contracted alpha (Azzi et al., 2014) and shortened free-running period upon release into constant conditions (Azzi et al., 2014; Schwartz et al., 2011). However, unlike photoperiodic after-effects, in which the changes in the period of the explanted SCN itself match those on behavior, there is a negative correlation between behavioral and SCN explant period following entrainment to T cycles. Exposure to short T cycles results in a long SCN free-running period and exposure to long T cycles results in a short SCN free-running period (Aton et al., 2004; Azzi et al., 2017; Molyneux et al., 2008).

The findings described above reveal a potential pattern of circadian after-effects, with long photoperiods and short T cycles producing one set of behavioral responses (short alpha, short tau), and short photoperiods and long T cycles producing another (long alpha, long tau). This alignment is particularly appealing, as recent work has revealed a role for DNA methylation in establishing period after-effects of extended T cycle entrainment, providing a promising biochemical mechanism for these changes (Azzi et al., 2014). The linkage between the two types of after-effects, however, has not yet been sufficiently interrogated. The discordance between the SCN after-effects of T cycle and photoperiod offers a hint that the relationship may not be so simple. Here, we seek to further examine the alignment of T cycle and photoperiodic after-effects by measuring the *in vivo* response of alpha, tau, and psi along with the *ex vivo* SCN response of phase distribution, tau, and psi following exposure to six combinations of photoperiod length and T cycle. We find that after-effects in each of these rhythm characteristics respond to the six different light cycles in distinct patterns, suggesting that they are each induced by different aspects of the input light cycle. Using skeleton photoperiods, we demonstrate that parametricity differs between after-effects in activity duration, period and psi, further indicating encoding of distinct components of light input by each of these characteristics. Examining the rhythms of explanted SCN *ex vivo* following entrainment to these light schedules, we find that the pattern of SCN phase dispersal reflects that of alpha *in vivo*, providing additional correlative evidence that SCN phase distribution may be a determining factor in setting activity duration.

MATERIALS AND METHODS

Animals

Animal experiments were conducted in accordance with Vanderbilt University Institutional Animal Care and Use Committee regulations. All animals used for behavioral experiments were heterozygous for the *Per2::Luciferase* allele (*Per2::Luciferase*$^{+/-}$) or were *Per2* wild-type (*Per2::Luciferase*$^{-/-}$). All animals used for SCN slice culture experiments were heterozygous for the *Per2::Luciferase* allele (*Per2::Luciferase*$^{+/-}$).

Activity Monitoring and Housing

Animals were singly-housed in light-tight boxes with activity monitoring by wheel revolutions detected by ClockLab acquisition software (Actimetrics, Inc.). Complete photoperiods used were 15:8 and 16:7 (T23 Long, ~67%), 8:15 and 7:16 (T23 Short, ~33%), 16:8 (T24 Long, ~67%), 8:16 (T24 Short, ~33%), 17:9 (T26 Long, ~67%), and 9:17 (T26 Short, ~33).

Animals were transferred to the specified light schedule after at least 3 weeks of age, and housed there for at least 28 days before transfer to DD or brain extraction for slicing. Six T26 Short animals included in the datasets (three used in behavioral experiments, three used in slice experiments) experienced a multi-hour light failure during the 28 days of entrainment, but received 14 days of the correct light cycle following the failure.

Skeleton photoperiods were set up by housing animals in 12:12 LD complete photoperiods for approximately 5 days before transitioning to a 12:12 skeleton (1:10:1:12 L:D:L:D). After several cycles on this skeleton, the onset pulse was gradually advanced (0.5 hour – 1 hour per day) or delayed (1 hour per day) until a skeleton long (1:14:1:8 L:D:L:D) or skeleton short (1:6:1:16 L:D:L:D) photoperiod, respectively, was established. Once the final skeleton was established, animals were given 28 days of exposure to that skeleton until transfer to DD or slicing.

Actogram Analysis

Locomotor behavior was analyzed using ClockLab Analysis software and R. Period was determined using chi square periodogram over the first 7 days of DD. Alpha was measured

using automated onset/offset detection for each cycle of the actogram. Full actograms can be found in Supplemental Data 1.

Automated Alpha Measurement

Automated alpha measurement was performed in R. The activity (bin size 6 minutes) is smoothed by a Savitzky-Golay filter with a span of 25 and degree of 3. A threshold is set relative to the maximum smoothed activity (0.01 * the maximum for day-by-day, 0.1 * the maximum for average profile). Points at which the smoothed activity crosses this threshold are identified as potential onsets and offsets. Segments of activity less than 2 hours are considered inactive. The longest inactive segment is identified, with the start of that segment recorded as the offset and the end of that segment recorded as the onset. Alpha is calculated as activity offset – onset, and psi as the timing of the activity onset in the first cycle in DD relative to the projected time of lights off from the previous light dark cycle (projected Zeitgeber Time 12 [ZT12]). Identified onsets and offsets for each cycle can be found in Supplemental Data 2. R scripts used for analysis can be found at 10.6084/m9.figshare.11513892.

Slicing and Slice Cultures

Within 4 hours of lights off, animals were sacrificed by cervical dislocation and the brain removed. SCN slices of 200-µm were made, and the SCN further isolated by scalpel cut under a dissecting microscope. Slices were transferred to a 6-well plate with cell culture membrane insert (Millipore, PICMORG50) and 1.2-mL of slice culture media. Slice chambers were sealed with a coverslip and vacuum grease and placed into an incubated light-tight inverted microscope (Zeiss Axioskop). Luminescence was detected using an intensified CCD (Stanford Photonics) controlled by µ-Manager recorded for 2’ every 10’ for at least 1 week.

Ex-Vivo Analyses

Luminescence recordings were analyzed using Fiji and R. OME-TIFF files from μ-Manager were opened in Fiji and smoothed using a two-frame minimization (frame rate reduction from 6/hour to 3/hour). A 102x102 grid of 10x10-pixel (5.175 x 5.175 μm) ROIs was overlaid on the images and brightness measured for each of these 10,404 ROIs measured for every frame. These grid measurements were then exported to R for further analysis. The first 8 hours of recording were excluded from peak-finding to prevent slicing artifacts from interfering with measurements. First, the ROIs comprising the SCN were identified by using pixels within the top 50% of brightness. The timing of each peak of luminescence was then detected for each ROI and used to calculate the initial phase. Distribution measurements were made by median absolute deviation across all SCN ROIs. Phase maps of each SCN used can be found in Supplemental Data 3. R scripts used for analysis can be found at 10.6084/m9.figshare.11513892.

RESULTS

Distinct response patterns of psi, and after-effects on alpha and period

To examine the persistent encoding of photoperiods and T cycles *in vivo*, as represented by entrained phase angle (psi) and after-effects in activity duration (alpha) and free-running period, we exposed mice to six different light schedules consisting of combinations of short or long photoperiod and short, standard, and long T cycles (T23 Long, T23 Short, T24 Long, T24 Short, T26 Long, T26 Short, Figure 1A). Following 14-28 days of exposure to these light schedules (see Methods), animals were transferred into constant darkness (DD) for 7 days. Based on previous studies examining the after-effects of T cycles (Azzi et al., 2014, 2017; Pittendrigh and Daan, 1976a; Schwartz et al., 2011) and photoperiod (Buijink et al., 2016; Ciarleglio et al., 2009; Evans et al., 2013; Pittendrigh and Daan, 1976a), we hypothesized that the response of period and alpha after-effects to these six light schedules would produce one of three general patterns (Supplemental Figure S1).

First, if after-effects in these rhythm characteristics were strictly dependent on the duty cycle of the light interval, then the groups would segregate into two levels, corresponding to long or short photoperiods, regardless of T cycle (Supplemental Figure S1A). A primary influence of the photoperiod could indicate a parametric effect of the total light phase duration per cycle and/or a non-parametric effect from the phase shifts caused by light onset and light offset. Second, if plasticity is strictly dependent on net daily phase advances or delays driven by entrainment to the T cycles, then the measurements would segregate into three groups based on T cycle (Supplemental Figure S1B). This pattern of results would most readily suggest that after-effects were induced by non-parametric effects of the daily entraining phase shifts induced by the T cycles. Third, significant main effects of both T cycle and photoperiod would result in after-effects with each of the 6 groups having a characteristic level (Supplemental Figure S1C),

while interactions between T cycles and photoperiod would produce many possible variations of the pattern in S1C.

Indeed, phase angle of entrainment of locomotor rhythms relative to projected ZT12 of the previous light:dark cycle (Methods) was strongly influenced by both T cycle length and photoperiod length, with a significant interaction between these two main effects (Figure 1B). As T cycle length increases, phase angle becomes more advanced. Within each T cycle, the short photoperiod version produces a more delayed phase angle than its long photoperiod counterpart, but the difference between the two photoperiods decreases as T cycle length increases. This pattern resembled the example in Supplemental Figure S1C, with the interaction providing an additional layer of complexity. In contrast to the multifaceted inputs to phase angle, we found that photoperiod was the sole significant influence on alpha, with persistently reduced activity duration in DD following long photoperiods compared to short photoperiods across all three T cycles (Figure 1C). This pattern most closely resembled the example in Supplemental Figure S1A, and suggested that a parametric effect of the duration of light per cycle and/or a non-parametric effect of the phase shifts caused at light onset and offset induced the after-effect in alpha. After-effects on locomotor period were significantly influenced by both T cycle length and photoperiod (Figure 1D), but unlike phase angle, there was no detectable interaction between the main effects. Within each T cycle, the long photoperiod group had consistently shorter free-running period compared to its partner short photoperiod. Between T cycles, however, there was a direct relationship between the T cycle length and the free-running period with free-running period increasing along with T cycle period regardless of photoperiod. This pattern most closely resembles the example in Supplemental Figure S1C.

To further examine the relationship between the alpha and period after-effects, we plotted the two measurements against one another (Figure 2). The two factors correlated significantly in two specific cases: T23 Long (Figure 2, top left) and T26 Short (Figure 2, bottom

right). These two photoperiod/T cycle combinations represent the instances where in previous reports T cycle and photoperiod independently produce similar *in vivo* after-effects on alpha and period, with long photoperiod or short T decreasing alpha and period, and short photoperiod or long T increasing alpha and period. Interestingly, there was a lack of correlation of these measures in T cycle/photoperiod combinations where the predicted after-effects of the cycle period and photoperiod would be in nominal conflict (Long photoperiod and Long T, and Short photoperiod and Short T, Azzi et al., 2014; Pittendrigh and Daan, 1976a).

Phase and alpha after-effects differ in their parametricity

The after-effects described in Figure 1 for all parameters showed significant main effects of photoperiod, revealing that either the interval between light transitions, or the light duration is inducing persistent effects on phase angle, activity duration, and period. To determine whether the critical aspect of the light cycle is the timing of the light/dark and dark/light transitions, or the duration of light within each cycle, we used skeleton long or short photoperiods consisting of two 1-hour pulses of light, separated by intervals of darkness, that mimic the timing of the light/dark transitions on full photoperiods of 16:8 and 8:16 (Figure 3A). Skeleton photoperiods have been used to assess the mechanism of entrainment through seasonal changes in phase angle (Pittendrigh and Minis, 1964), as well as to determine the proximal effect on locomotor behavior duration (Pittendrigh and Daan, 1976a, 1976b). In order to determine whether skeleton photoperiods can induce plasticity in alpha, period, and phase angle, we assessed after-effects in locomotor behavioral rhythms in DD following 28 days of exposure to skeleton long or short photoperiods, in comparison to similar entrainment to full 16:8 and 8:16 photoperiods.

Phase angle of entrainment exhibited main effects of both the duration of light in complete photoperiods (Completeness, Figure 3B), and the timing of light transitions in skeleton photoperiods (Interval, Figure 3B). This result demonstrates that the phase angle of entrainment induced by photoperiodic entrainment has a significant non-parametric component. In addition

to the main effect of the interval between light transitions on skeleton photoperiods, there is also a significant effect of the light duration of complete photoperiods, indicating that there is a parametric influence on the phase angle of entrainment of locomotor behavior rhythms. In contrast, we found a significant main effect only of the onset-offset interval of skeleton photoperiods on alpha after-effects, suggesting that this effect is primarily non-parametric (Figure 3C). We found that the skeleton photoperiods had no significant effect on period (Figure 3D), however previous investigators have reported modest period after-effects of skeleton photoperiods (Pittendrigh and Daan, 1976a). Thus we found that there are significant parametric and non-parametric effects on phase angle of entrainment, non-parametric effects of onset-offset interval on alpha, and relatively weak non-significant after-effects on period of skeleton photoperiods.

***Ex vivo* SCN after-effects**

Using the same six light schedules described above, we investigated the effects of photoperiodic light exposure on plasticity of the SCN pacemaker, using *ex vivo* imaging of PER2::LUCIFERASE (PER2::LUC) rhythms. We housed heterozygous PER2::LUC animals in identical conditions to our complete photoperiod *in vivo* experiments, including running wheels, and collected SCN slices from the animals after 14-28 days of exposure to each of the light schedules described above. Slices were collected within 4 hours of lights off, maintained in organotypic culture, and PER2::LUC luminescence recorded *ex vivo* for 5-7 days (see Methods). Slice recordings were analyzed by spreading a 102 x 102 grid of sub-cellular (~5 x 5 μm) regions of interest (ROIs) across the entire image, and then analyzing each SCN ROI for its PER2::LUC peak times. These PER2::LUC peak times were then used to calculate phase distributions and create phase maps (Figure 4A), while the average PER2::LUC luminescence profile over time was used to calculate SCN period.

We found that the phase angle of SCN PER2::LUC rhythms referenced to projected ZT12 of the previous light cycle was significantly influenced by both T cycle and photoperiod, with a significant interaction between the two factors (Figure 4B), similar to the phase angle of entrainment of locomotor rhythms. As T cycle length increases, SCN phase angle also becomes more advanced, and within each T cycle the long photoperiod is more advanced than the short. Again, like the *in vivo* phase angle, the *ex vivo* phase angle featured a narrowing difference between long and short as T cycle length increases. Similarly, mirroring *in vivo* alpha, we found that the photoperiod modulated the degree of synchrony of PER2::LUC rhythms within explanted SCN (phase distribution, Figure 4C), with increased phase dispersion in long photoperiods compared to short. However, we also found a significant main effect of T cycle length on the SCN phase distribution after-effect. This effect was driven by increased phase dispersal in both T26 groups compared to both T24 groups (post-hoc multiple comparisons test between T cycle lengths, T24 vs. T26 adjusted $p = 0.0329$). There is no single consistent linear effect of T cycle on the *ex vivo* phase distribution after-effect. As such, the pattern most resembled that of the example in Supplemental Figure 1A, but with the T26 groups elevated.

SCN period after-effects following T cycle entrainment have been a source of significant interest in part because of the apparent disconnect between after-effects of T cycle (where *ex vivo* SCN and behavioral measurements negatively correlate) and after-effects of photoperiod (where *ex vivo* SCN and behavioral measurements agree). In our combined T cycle/photoperiod paradigm we found a significant negative relationship between T cycle length and SCN period length. Entrainment to short T cycles *in vivo* resulted in lengthened SCN period *ex vivo*, and *vice versa* as previously reported (Aton et al., 2004; Azzi et al., 2017; Molyneux et al., 2008). Visually, there is an intriguing reversal in trend direction of possible photoperiod effects between T24 and the two non-24 T cycles, that could indicate an interaction. In T24 cycles, the previously reported relationship between long and short photoperiod (shortened, behavior-like

period after-effect for long photoperiod) is present, while in T23 and T26 cycles, the relationship between long and short is inverted. This relationship results in the longest and shortest periods aligning with T23 Long and T26 Short, the same two groups highlighted above (Figure 2) as overlap groups where the effects of T cycle and photoperiod are in line with one another. However, no significant photoperiod effects or interactions were revealed by the ANOVA, or by multiple post-hoc tests for differences within the T cycle groups, so these visual trends require further testing.

***Ex vivo* SCN after-effects have similar parametricity to behavioral after-effects**

To investigate the parametricity of SCN after-effects *ex vivo*, we collected slices from animals entrained to skeleton long and short photoperiods (Figure 5A). Similar to *in vivo* phase angle of entrainment of the behavioral rhythm to skeleton photoperiods, there was a significant effect of skeleton onset-offset interval on the phase angle of the PER2::LUC rhythm (Figure 5B). Unlike *in vivo*, the PER2::LUC phase angle did not have a significant effect of photoperiod completeness, although there was a trend towards a decrease in the effect size on phase angle of skeleton photoperiods compared to the complete photoperiods. The phase distribution after-effect was significantly influenced by the onset-offset interval (Figure 5C), similar to *in vivo*. The phase distribution after-effect *ex vivo* was also significantly influenced by photoperiod completeness. However, the effect size of the skeleton photoperiods on SCN phase distribution was larger compared to the complete photoperiods. Though the interaction that this implies was not statistically significant, it does suggest that skeleton interval is a principal driver of phase distribution after-effects similar to *in vivo* alpha (Figure 3C). As with behavioral period after-effects, we found no significant effect of onset-offset interval or photoperiod completeness on the *ex vivo* period after-effect, again suggesting that the effects of photoperiod on period after-effects are modest compared to T cycle entrainment.

DISCUSSION

We examined the relative influences of T cycle period, photoperiod, and onset-offset interval on phase angle of entrainment, as well as on after-effect responses of alpha, period, and phase distribution within the SCN. Using eight light cycle input groups, including six T cycle/photoperiod combinations and two skeleton photoperiods, we intended to test which specific components of light cycle input (light duration, onset-offset interval, repeated phase shifts) are encoded in a persistent manner in the SCN as implied by expressed as after-effects in circadian behavior, and in SCN rhythms assayed *ex vivo*.

We found that phase angle of entrainment is strongly influenced by T cycle and photoperiod length, both *in vivo* (Figure 1B) and *ex vivo* (Figure 4B), with increasing T cycle length being associated with more advanced phase angle, and long photoperiods having more advanced phase angle than their short photoperiod counterparts. There was also a significant interaction between T cycles and photoperiod in setting subsequent phase, both *in vivo* and *ex vivo*. Both *in vivo* and *ex vivo*, the difference in phase angle between short and long photoperiods decreased in T26. Using skeleton photoperiods *in vivo* and *ex vivo*, we found the determination of phase angle difference between long and short photoperiods *in vivo* to exhibit both significant non-parametric (light onset-offset interval), and parametric components (completeness, Figure 3B), while the phase of the *ex vivo* SCN also exhibited a significant non-parametric main effect of onset-offset interval, and a trend toward a parametric effect (see description of results in Figure 5B). Determination of phase has long been considered to be non-parametric, with the exception of the continuity of light on full light cycles disambiguating onset from offset on near symmetrical light cycles (e.g. near T24 12:12) (Pittendrigh and Minis, 1964), however our results suggest a more complex picture more akin to the circadian surface entrainment model of Roenneberg for *Neurospora* (Rémi et al., 2010; Roenneberg et al., 2010).

After-effects in activity duration, or alpha, were strongly influenced by photoperiod length (Figure 1C) in a non-parametric manner (Figure 3C). This was mirrored by the significant main effect of photoperiod on *ex vivo* SCN phase distribution, a measure that is akin to activity duration for the SCN slice (Figure 4C) that was also primarily non-parametric in that it was driven by onset-offset interval (Figure 5C). One notable difference between *in vivo* alpha and *ex vivo* SCN phase distribution, however, was the general increase in SCN phase dispersal measured in both photoperiods of the T26 group. One possible explanation for this increase in the T26 Short group may be the contracted proximal alpha observed in LD during entrainment to T26 Long and Short (Figure 1A, bottom row). Though the free-running alpha expands on the first day of DD, there is some apparent negative masking occurring in the early active phase of these mice during LD. Because slices are made during the last LD cycle rather than on the first day of DD, the phase distribution could reflect that negatively-masked pattern and imply that phase distribution is correlated with overt “net” alpha, rather than the underlying assumed endogenous active phase length.

We find that behavioral period after-effects are significantly influenced by both T cycle and photoperiod length, but that the T cycle influence is of greater statistical significance and effect size (Figure 1D), suggesting that the T cycle input to period after-effects is more robust than photoperiod. Our results with skeleton photoperiods *in vivo* support this notion, as we did not observe significant period after-effects with skeleton photoperiods (Figure 3D). It is worth noting that some investigators have observed period after-effects of skeleton photoperiods on behavioral period, but with modest effect sizes (Pittendrigh and Daan, 1976a). We observed period changes in *ex vivo* SCN explanted from mice entrained to non-24 hour T cycles that negatively correlated with the period of the entraining T cycle, and the changes in behavioral free-running period, consistent with previous findings (Aton et al., 2004; Azzi et al., 2017; Molyneux et al., 2008). We did not detect any statistically significant modulation of the T cycle

effects on period by varying photoperiod, but visually, there are trend reversals in the expected direction of photoperiodic effects on period in the non-24 hour T cycle groups that suggest the possibility of interactions that we did not detect statistically (T24 Long vs. T23 Long, $p = 0.1513$; T24 Short vs. T26 Short, $p = 0.0584$; Sidak's Multiple Comparisons).

Because alpha and period after-effects have been observed together (shorter alpha, shorter period; longer alpha, longer period), there have been attempts to explain both changes with a single underlying mechanism (Beersma et al., 2017; Gu et al., 2016). As we report here, however, period and alpha can change together in a correlated manner under some combinations of T and duty cycle, or separately (Figure 2), and so it follows that the mechanisms underlying those changes may be distinct. We observed different patterns of responses for after-effects in alpha and period in photoperiod/T cycle combinations (Figure 1A, C-D) as well as in skeleton photoperiods (Figure 3A, C-D), and correlation of changes in alpha and period were specific to certain T and photoperiod combinations (Figure 2). When measuring the correspondence of period and alpha after-effects *in vivo*, correlations were only observed in cases where T cycle and photoperiod effects are expected to align (Figure 2). These results suggest that while the two after-effects may frequently be observed together, their distinct patterning in response to particular T cycles and photoperiods could be driven by disparate but conditionally convergent mechanisms.

Changes in SCN phase dispersal remains a likely candidate for alterations in downstream locomotor behavior duration, as an extended population-level high-firing phase of SCN neurons, for which the clock gene (PER2::LUC) phase distribution is a proxy here, would logically underlie the regulation of timing activity or inactivity (Ciarleglio et al., 2009, 2011; Inagaki et al., 2007; VanderLeest et al., 2007). Changes in period, however, shown here to be induced primarily through T cycle entrainment and likely the accompanying repeated phase shifts thereof, may be regulated in a different manner. Mechanisms suggested recently by other

groups (Azzi et al., 2014, 2017) surrounding the epigenetic changes that may occur after extended entrainment to T cycles may help explain alterations in the free-running period that we observed.

Regional phase differences within the SCN network have been observed in response to T cycles and photoperiod, and have been proposed to drive period after-effects (Azzi et al., 2017; Buijink et al., 2016; Evans et al., 2013; Myung et al., 2015). In SCN explants from mice entrained to long photoperiods, there is increased phase lead of the ventral or ventromedial region of the SCN in some studies (Buijink et al., 2016; Evans et al., 2013), but the reverse regional phase relationship was observed in another study (Myung et al., 2015). In these studies, SCN period shortening after entrainment to long photoperiods was observed to correlate with ventral phase lead (Evans et al., 2013), with ventral phase lag (Myung et al., 2015), or not be present (Buijink et al., 2016). Similarly, Azzi *et al*. (2017) found that following entrainment to T cycles, there was an anticorrelation between SCN period after-effect and the previous T cycle period, as expected from previous results (Aton et al., 2004; Molyneux et al., 2008). The same study also found regional phase differences such that shortened period correlated with ventral phase lag, while lengthened period correlated with ventral phase lead – the opposite pattern previously found for photoperiodic period after-effects by the same group (Evans et al., 2013). Thus, there is no clear consensus in the literature as to whether SCN regional phase differences mediate period after-effects. We also observed the anticorrelation of *ex vivo* SCN period after T cycle entrainment *in vivo*, and we observed a variety of regional phase distributions across our experimental conditions that included examples of ventral core phase lead in response to short T cycles similar to Azzi *et al*. (2017) (see T23 Long in Figure 5), and examples of more ventromedial phase clustering similar to that of Buijink *et al*. (2016) in response to long T cycles (see T26 Short in Figure 5). We speculate that the lack of clarity in

our data and the published results with respect to regional phase patterns and SCN period may arise from both technical and conceptual issues.

Technically, differences in regional patterns (ventral core vs. ventromedial) may be explained by slice position on the rostral caudal axis of the SCN. Azzi et al. (2017) in their supplement show that taking sections more caudal in the SCN changes the regional phase pattern from ventral core grouping to a ventromedial grouping similar to Buijink (2016). We speculate that we may have not controlled well enough for slice depth, resulting in our observation of variations of both patterns in our data. Conceptually, the anticorrelation of SCN *ex vivo* period with *in vivo* period after-effects of T cycles presents a challenge. One interpretation of these results is that the observed *ex vivo* period represents a deafferentation-induced reorganization of the SCN network upon explantation, indicating extra-SCN input is key to T cycle after-effects *in vivo* (Aton et al., 2004; Molyneux et al., 2008). Support for this view comes from our previous results showing an anticorrelation between *in vivo* behavioral and *ex vivo* SCN period effects of genetic serotonergic de-afferentation of the SCN (Ciarleglio et al., 2014). In addition, part of the confound regarding previous *ex vivo* SCN T-cycle after-effects also appears to be a bias in the reporting of SCN regional rhythms by the standard PER2::LUC reporter that more highly weights period of the dorsal region (Azzi et al., 2017). In any case, the lack of correspondence between *in vivo* and *ex vivo* T-cycle period after-effects in the SCN makes it difficult to attribute *ex vivo* findings of regional patterns or mechanisms to the *in vivo* case, although the system can be used to study SCN *ex vivo* reorganization and its mechanisms (Azzi et al., 2017).

Measurements in constant conditions reveal properties of the SCN and downstream circadian outputs free of light input, and as such the study of after-effects is one means to understand the plasticity of the SCN in response to seasonal light conditions. Understanding after-effects is also useful *per se*, as the encoding of light information within the SCN allows

seasonal circadian properties to remain stable across ephemeral changes in the environment. Organisms in the wild experience fluctuations in light exposure during the annual photoperiodic cycle because of weather, nesting, hibernation, and other factors. Stable but flexible encoding of seasonal light inputs within the circadian system would allow for consistency across these light exposure fluctuations.

Changes to SCN network synchrony may also have additional ramifications in the form of altered responses to light input, potentially explaining previously observed larger phase shifts after exposure to short days, and smaller phase shifts after exposure to long days (Refinetti, 2002). The role of SCN neuron phase dispersal in mediating those altered responses and altered free-running period has been explored computationally (Gu et al., 2016) and through altered GABA signaling (Farajnia et al., 2014). In their analysis of after-effects on free-running period, Pittendrigh and Daan (1976b) suggested that this change in circadian property may provide functional significance in terms of priming future responses to light, but it remains to be seen whether any of these after-effects constitutes an adaptive advantage or if they are simply a side effect of altered network synchrony.

Because current methods for *in vivo* imaging are limiting, the measure of activity duration after-effects may be a useful proxy for inferring the waveform of the SCN. The integrity of this SCN waveform/activity duration connection depends on the correlation between the two. Our findings that alpha and *ex vivo* SCN neuron phase dispersal associate across multiple lighting conditions regardless of net daily phase shift do not address causality, but strengthen the association between the two measurements. As the broadened electrical waveform of the SCN is associated with the compressed behavioral activity duration seen in long photoperiods (and the contracted waveform with extended activity duration in short photoperiods), the spread in phase of SCN neurons and the corresponding widening of overall firing that occurs as a result should account for the observed changes in activity duration (Houben et al., 2009).

The degree of SCN neuron phase dispersal is a characteristic attribute of photoperiodic encoding, as it represents a change in state of the SCN that is induced by the duration of the light interval of the light cycle and then is maintained after transfer to constant conditions (Buijink et al., 2016; Ciarleglio et al., 2011; Inagaki et al., 2007; VanderLeest et al., 2007). Our results here suggest that the timing of light/dark transitions is a key factor in influencing SCN phase dispersal (Fig. 5C) underlying encoding of *in vivo* activity duration (Fig. 3C), although we also detected an effect of light duration on SCN phase distribution (Fig. 5C). The spread in the timing of neuronal rhythms allows for the overall high firing phase of the SCN to be broadened or contracted without required alteration to the waveforms of individual SCN neurons although this aspect is modulated by developmental inputs (Ciarleglio et al., 2011). As such, the degree of phase distribution within the SCN is a potential target for artificial SCN manipulation – driving neurons to adopt the phase distribution characteristic of a photoperiod, such as by pharmacologically, optogenetically, or chemogenetically extending the high firing phase, would be expected to induce the behavioral activity duration characteristic of that particular photoperiod, and perhaps other photoperiod-dependent responses, such as reproductive state and affective behaviors.

Taken together, our results show that distinct components of light cycles can have likewise distinct effects on the circadian system, with the timing of light/dark transitions in photoperiods driving plasticity in alpha, photoperiod and T cycle length combining to drive plasticity in period and phase of *in vivo* behaviors and gene expression in the *ex vivo* SCN, and phase distribution within the *ex vivo* SCN being affected by light/dark transition interval and long T cycle lengths. These results open the door to selective manipulation of circadian plasticity in activity duration or period for experimentation or therapy. The results shown here also demonstrate the utility of deconvolving overlapping types of input when studying complex processes within the SCN. Our results indicate that alpha and period after-effects are possibly

driven by distinct, though perhaps related, mechanisms, and such information can be incorporated into experimental and computational approaches to test the system in the future. With new techniques currently being established in our field to measure SCN neuronal firing rate, calcium signaling, and activity levels with high cellular specificity and extended timeframe, there will be an improved ability to characterize the specific effect of photoperiodic influences on these circadian components.

ACKNOWLEDGMENTS

The authors would like to thank Maria Luísa Jabbur, Carl Johnson, Terry Page, and Chloe Snider for their helpful comments and discussions. This work was supported by NIH R01 GM117650 to D.G.M., NIH F31 NS096813 to M.C.T., and NSF GRFP 0909667 to M.C.T.

AUTHOR CONTRIBUTIONS

M.C.T. and D.G.M conceived the experiments. M.C.T. performed the experiments. M.C.T. and J.C.H. analyzed the data, M.C.T., J.C.H., and D.G.M. wrote the paper.

DECLARATION OF INTERESTS

The authors have no competing interests to report.

REFERENCES

Aton SJ, Block GD, Tei H, et al. (2004) Plasticity of circadian behavior and the suprachiasmatic nucleus following exposure to non-24-hour light cycles. *J Biol Rhythms* 19(3): 198–207.

Azzi A, Dallmann R, Casserly A, et al. (2014) Circadian behavior is light-reprogrammed by

plastic DNA methylation. *Nature Neuroscience* 17(3): 377–382.

Azzi A, Evans JA, Leise T, et al. (2017) Network Dynamics Mediate Circadian Clock Plasticity. *Neuron* 93(2): 441–450.

Bartness TJ and Wade GN (1984) Photoperiodic control of body weight and energy metabolism in syrian hamsters (mesocricetus auratus): Role of pineal gland, melatonin, gonads, and diet. *Endocrinology* 114(2): 492–498.

Bartness TJ, Elliott JA and Goldman BD (1989) Control of torpor and body weight patterns by a seasonal timer in Siberian hamsters. *American Journal of Physiology-Regulatory, Integrative and Comparative Physiology*.

Basnet S, Merikanto I, Lahti T, et al. (2016) Seasonal variations in mood and behavior associate with common chronic diseases and symptoms in a population-based study. *Psychiatry Research*.

Beersma DGM, Gargar KA and Daan S (2017) Plasticity in the Period of the Circadian Pacemaker Induced by Phase Dispersion of Its Constituent Cellular Clocks. *Journal of Biological Rhythms* 32(3): 237–245.

Buijink MR, Almog A, Wit CB, et al. (2016) Evidence for weakened intercellular coupling in the mammalian circadian clock under long photoperiod. *PLoS ONE* 11(12).

Ciarleglio CM, Gamble KL, Axley JC, et al. (2009) Population encoding by circadian clock neurons organizes circadian behavior. *The Journal of neuroscience□: the official journal of the Society for Neuroscience* 29(6): 1670–1676.

Ciarleglio CM, Axley JC, Strauss BR, et al. (2011) Perinatal photoperiod imprints the circadian clock. *Nat Neurosci* 14(1). Nature Publishing Group: 25–27.

Ciarleglio CM, Resuehr HES, Axley JC, et al. (2014) Pet-1 deficiency alters the circadian clock

and its temporal organization of behavior. *PLoS ONE*.

Elliott JA and Goldman BD (1981) Seasonal reproduction. In: *Neuroendocrinology of reproduction*. Springer, pp. 377–423.

Evans JA, Leise TL, Castanon-Cervantes O, et al. (2013) Dynamic interactions mediated by nonredundant signaling mechanisms couple circadian clock neurons. *Neuron* 80(4): 973–983.

Farajnia S, van Westering TLE, Meijer JH, et al. (2014) Seasonal induction of GABAergic excitation in the central mammalian clock. *Proceedings of the National Academy of Sciences* 111(26): 9627–9632.

Fernandez DC, Fogerson PM, Lazzerini Ospri L, et al. (2018) Light Affects Mood and Learning through Distinct Retina-Brain Pathways. *Cell*.

Gu C, Rohling JHT, Liang X, et al. (2016) Impact of dispersed coupling strength on the free running periods of circadian rhythms. *Physical Review E* 93(3): 032414.

Gwinner E (1990) Circannual rhythms in bird migration: control of temporal patterns and interactions with photoperiod. *Bird migration. Physiology and ecophysiology*: 257–268.

Houben T, Deboer T, Van Oosterhout F, et al. (2009) Correlation with behavioral activity and rest implies circadian regulation by scn neuronal activity levels. *Journal of Biological Rhythms*.

Inagaki N, Honma S, Ono D, et al. (2007) Separate oscillating cell groups in mouse suprachiasmatic nucleus couple photoperiodically to the onset and end of daily activity. *Proc Natl Acad Sci USA* 104(18): 7664–7669.

Koorengevel KM, Beersma DGM, den Boer J a, et al. (2003) Mood regulation in seasonal affective disorder patients and healthy controls studied in forced desynchrony. *Psychiatry*

research.

Mickman CT, Stubblefield JS, Harrington ME, et al. (2008) Photoperiod alters phase difference between activity onset in vivo and mPer2::luc peak in vitro. *American Journal of Physiology - Regulatory Integrative and Comparative Physiology*.

Molyneux PC, Dahlgren MK and Harrington ME (2008) Circadian entrainment aftereffects in suprachiasmatic nuclei and peripheral tissues in vitro. *Brain Research* 1228: 127–134.

Myung J, Hong S, DeWoskin D, et al. (2015) GABA-mediated repulsive coupling between circadian clock neurons in the SCN encodes seasonal time. *Proceedings of the National Academy of Sciences* 112(29): E3920–E3929.

Oh EY, Ansell C, Nawaz H, et al. (2010) Global breast cancer seasonality. *Breast Cancer Research and Treatment*.

Pittendrigh CS and Daan S (1976a) A functional analysis of circadian pacemakers in nocturnal rodents (I). *Journal of Comparative Physiology A* 106(3). Springer-Verlag: 223–252.

Pittendrigh CS and Daan S (1976b) A functional analysis of circadian pacemakers in nocturnal rodents (IV). *Journal of Comparative Physiology A* 106(3). Springer-Verlag: 291–331.

Pittendrigh CS and Minis DH (1964) The Entrainment of Circadian Oscillations by Light and Their Role as Photoperiodic Clocks. *The American Naturalist* 98(902): 261–294.

Refinetti R (2002) Compression and expansion of circadian rhythm in mice under long and short photoperiods. *Integrative Physiological and Behavioral Science*.

Rémi J, Merrow M and Roenneberg T (2010) A circadian surface of entrainment: Varying T, τ, and Photoperiod in Neurospora crassa. *Journal of Biological Rhythms*.

Roenneberg T, Rémi J and Merrow M (2010) Modeling a Circadian Surface. *Journal of*

Biological Rhythms.

Schwartz WJ, Tavakoli-Nezhad M, Lambert CM, et al. (2011) Distinct patterns of Period gene expression in the suprachiasmatic nucleus underlie circadian clock photoentrainment by advances or delays. *Proceedings of the National Academy of Sciences* 108(41): 17219–17224.

Tackenberg MC and McMahon DG (2018) Photoperiodic Programming of the SCN and Its Role in Photoperiodic Output. *Neural Plasticity* 2018: 1–9.

VanderLeest HT, Houben T, Michel S, et al. (2007) Seasonal Encoding by the Circadian Pacemaker of the SCN. *Current Biology* 17(5): 468–473.

Wehr TA (2001) Photoperiodism in humans and other primates: Evidence and implications. *Journal of Biological Rhythms*.

FIGURES

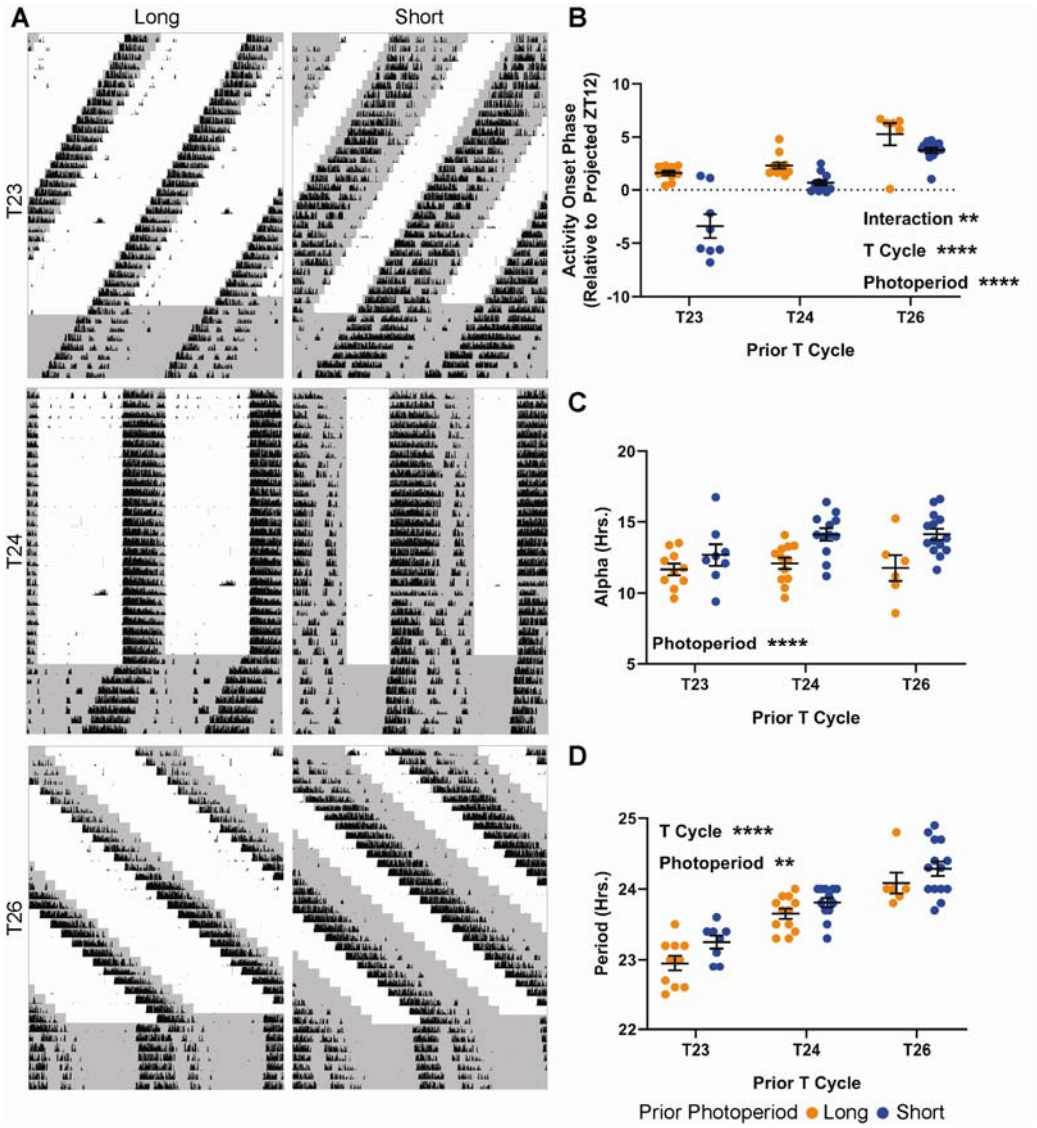

Figure 1. Behavioral after-effects of six photoperiod/T cycle combinations. **A**, representative actograms from long (left column) and short (right column) photoperiods combined with T23 (top row), T24 (middle row), and T26 (bottom row). **B**, phase angle of entrainment following exposure to the six light schedules. Values are relative to projected ZT12 (positive values advanced, negative values delayed). Interaction p = 0.0014 (7.242%), T Cycle Length $p < 0.0001$ (51.30%), Photoperiod Legth $p < 0.0001$ (20.97%). **C**, alpha after-effect across all six schedules as measured by automated alpha detection (see Methods). Interaction p = 0.4256 (2.081%), T Cycle Length p = 0.1648 (4.468%), Photoperiod Length $p < 0.0001$ (21.67%). **D**, period after-effect across the six schedules as measured by chi square periodogram. Interaction p = 0.7587 (0.2835%), T Cycle Length $p < 0.0001$ (56.17%), Photoperiod Length p = 0.0087 (3.778%).

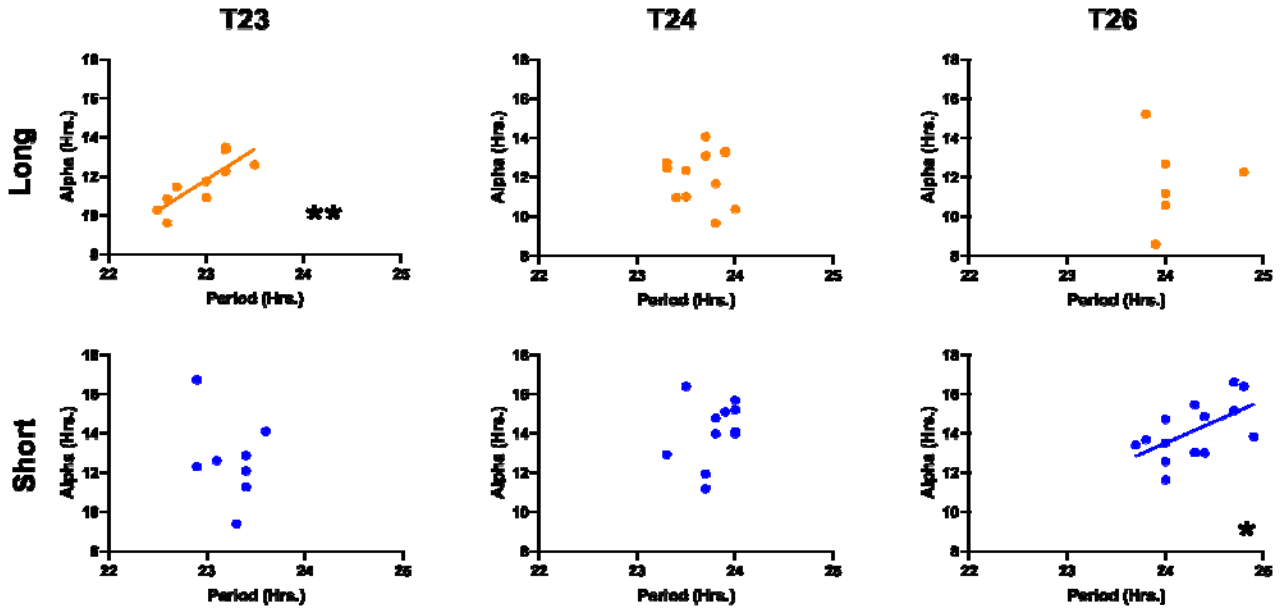

Figure 2. Within-individual correlations between period and alpha after-effects following the given T-cycle/photoperiod combination. T23 Long 0.8238 (0.0034, **), T24 Long -0.06835 (0.8328, ns), T26 Long 0.004966 (0.9926, ns), T23 Short -0.3147 (0.4477, ns), T24 Short 0.2671 (0.4013, ns), T26 Short 0.5818 (0.0291, *); Pearson r (*p* value).

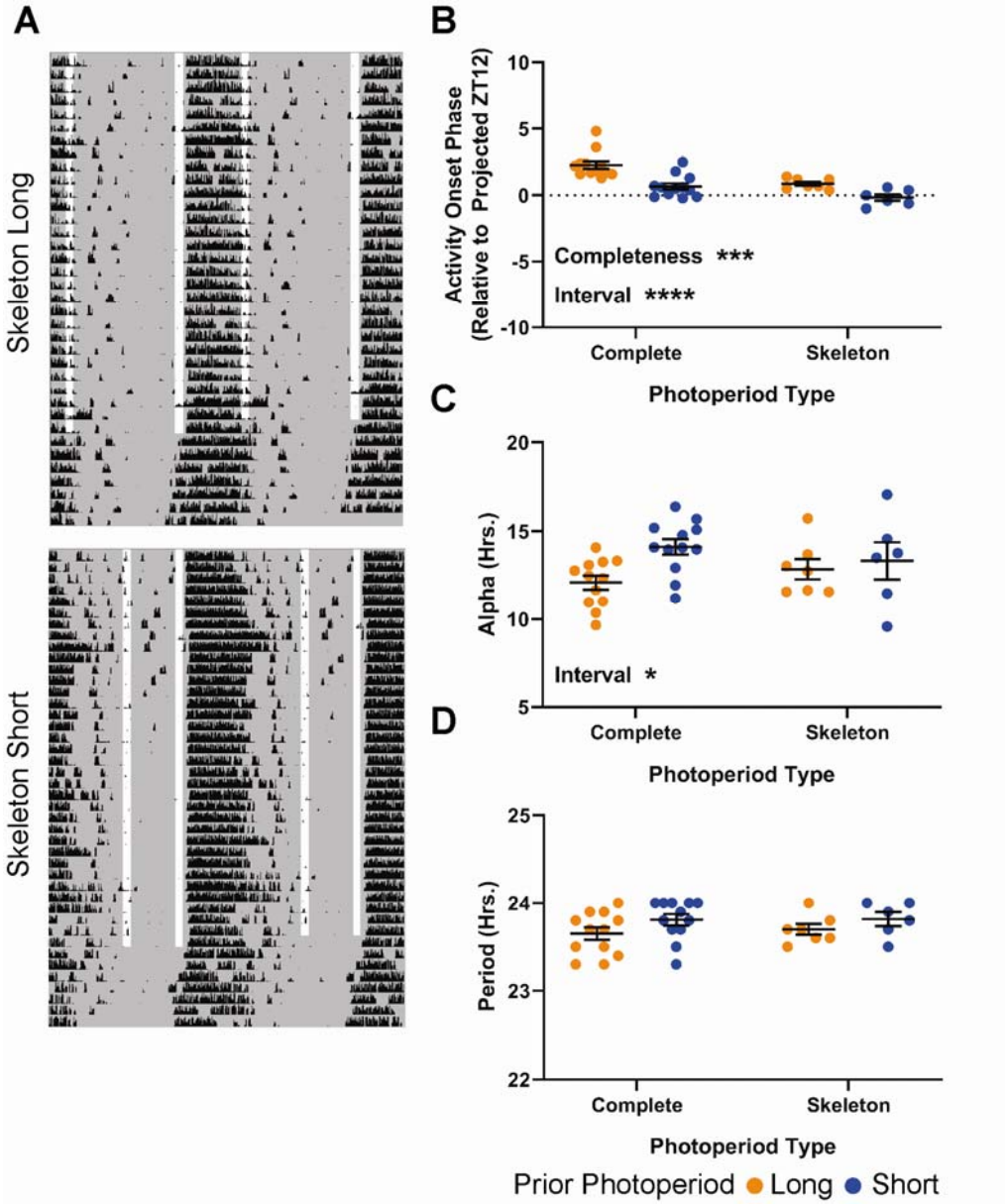

Figure 3. Behavioral after-effects following exposure to skeleton long and short photoperiods compared to T24 complete long and short photoperiods. **A**, representative actograms from long (top) and short (bottom) skeleton photoperiods. **B**, phase angle of entrainment following exposure to skeleton long and short photoperiods. Values are relative to projected ZT12 (positive values advanced, negative values delayed). Interaction p = 0.3161 (1.33%), Completeness p = 0.0003 (21.24%), Onset-Offset Interval p < 0.0001 (29.32%). **C**, alpha after-effect of skeleton long and short photoperiods. Interaction p = 0.1861 (4.332%), Completeness p = 0.9858 (0.0008%), Onset-Offset Interval p = 0.0376 (11.15%). **D**, period after-effect of skeleton long and short photoperiods. Interaction p = 0.7835 (0.2063%), Completeness p = 0.7006 (0.4044%), Onset-Offset Interval p = 0.0765 (8.988%). Long and Short complete photoperiod values in B-D are replotted from Figure 1.

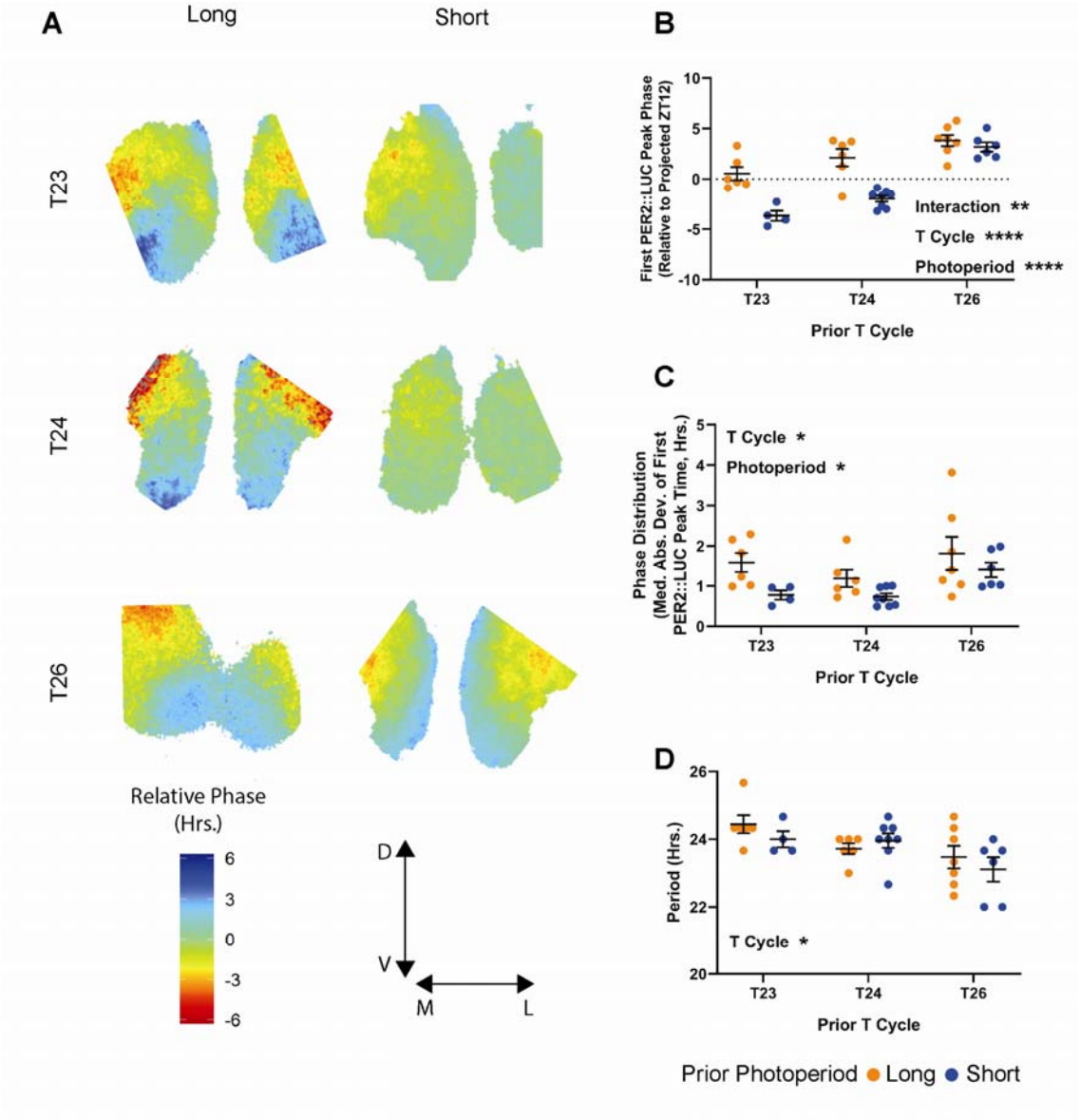

Figure 4. PER2::LUC after-effects following exposure to six photoperiod/T cycle combinations. **A**, representative relative phase maps from long (left column) and short (right column) photoperiod combined with T23 (top row), T24 (middle row), or T26 (bottom row). **B**, phase angle of entrainment of the PER2::LUC rhythm following entrainment to the specified T cycle/photoperiod combination. Values represent the time of the first PER2::LUC peak relative to the projected lights off for the first cultured cycle (projected ZT 12). Interaction $p = 0.0052$ (8.185%), T Cycle Length $p < 0.0001$ (49.47%), Photoperiod Length $p < 0.0001$ (24.94%). **C**, phase distribution (median absolute deviation of PER2::LUC peak times) across SCN slices from animals entrained to each of the specified light schedules. Interaction $p = 0.7168$ (1.433%), T Cycle Length $p = 0.0353$ (15.89%), Photoperiod Length $p = 0.0114$ (15.42%). **D**, period of the PER2::LUC rhythm over 5 cycles *ex vivo*. Interaction $p = 0.4104$ (4.109%), T Cycle Length $p = 0.0111$ (23.40%), Photoperiod Length $p = 0.4151$ (1.529%).

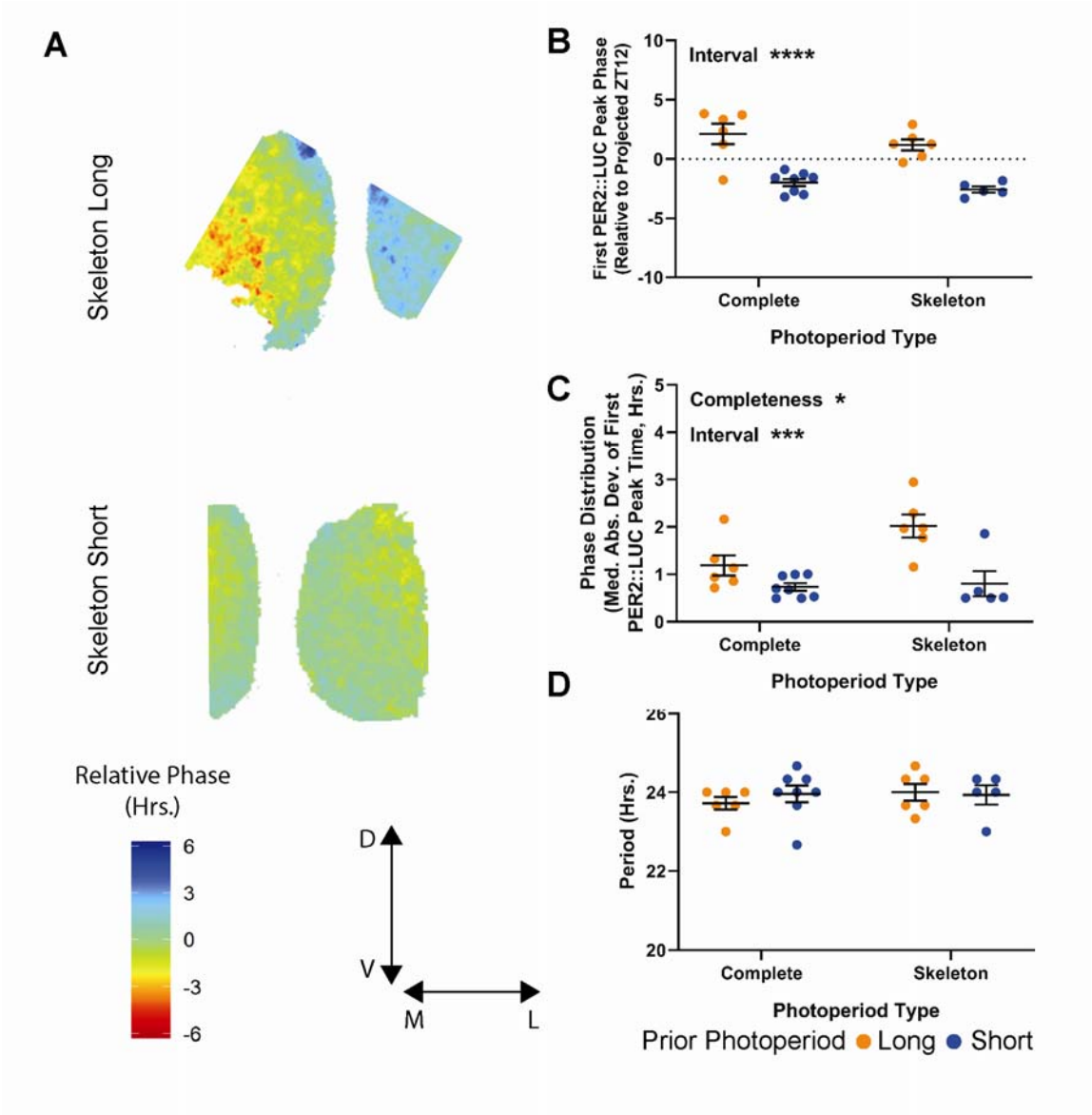

Figure 5. PER2::LUC after-effects following entrainment to skeleton long and short photoperiods compared to T24 complete long and short photoperiods. **A**, representative relative phase maps from skeleton long (top) and short (bottom) photoperiod. **B**, phase angle of entrainment of the PER2::LUC rhythm following entrainment to skeleton long and short photoperiods. Values represent the time of the first PER2::LUC peak relative to the projected lights off for the first cultured cycle (projected ZT 12). Interaction p = 0.7514 (0.1326%), Completeness p = 0.1660 (2.651%), Onset-Offset Interval p < 0.0001 (70.79%). **C**, phase distribution (median absolute deviation of PER2::LUC peak times) across SCN slices from animals entrained to skeleton long and short photoperiod. Interaction p = 0.0654 (7.695%), Completeness p = 0.0318 (10.77%), Onset-Offset Interval p = 0.0003 (37.26%). **D**, period of the PER2::LUC rhythm over 5 cycles *ex vivo*. Interaction p = 0.4867 (2.277%), Completeness p = 0.5608 (1.587%), Onset-Offset Interval p = 0.6959 (0.7131%). Long and Short complete photoperiod values in B-D are replotted from Figure 4.

SUPPLEMENTAL FIGURES

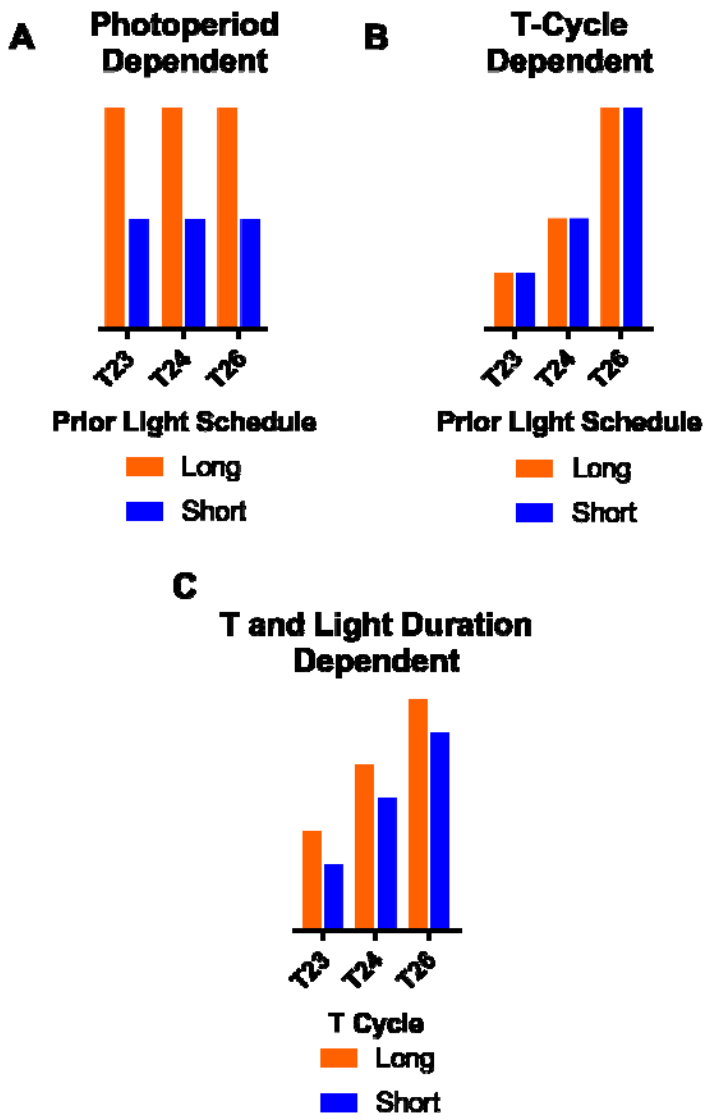

Supplemental Figure S1. Schematic of possible patterns of measurements across T23 L/S, T24 L/S, and T26 L/S. **A**, a T-cycle dependent response where the measurement is graded depending on the T cycle and photoperiod within the T-cycle has negligible effects. **B**, a photoperiod-dependent response where light duty cycle dictates the measurement regardless of T cycle. **C**, a combination of photoperiod and T cycle influences, with each of the 6 combinations having a characteristic measurement level. Note that in all examples, the polarity of the measurement change is arbitrary (e.g., T cycle response in A can increase or decrease with T cycle, photoperiod response in B can have either Long or Short measure higher).These patterns are illustrations of individual and combined main effects; possible interaction effects are not shown.